ETG Scale Turbulence and Transport in the DIII-D Tokamak

T.L. Rhodes 1), W.A. Peebles 1), M.A. Van Zeeland 2), J.S. deGrassie 3), R.V. Bravenec 4), K.H. Burrell 3), G.R. McKee 5), J. Lohr 3), C.C. Petty 3), X.V. Nguyen 1), E.J. Doyle 1), C.M. Greenfield 3), L. Zeng 1), and G. Wang 1)

1) University of California-Los Angeles, Los Angeles, California, USA
2) Oak Ridge Institute of Science Education, Oak Ridge, Tennessee, USA
3) General Atomics, San Diego, California, USA
4) University of Texas-Austin, Austin, Texas, USA
5) University of Wisconsin-Madison, Madison, Wisconsin, USA

e-mail contact of main author: rhodes@fusion.gat.com

Abstract. Small-scale density turbulence ($k_\perp \rho_i \sim$ 4-10) and electron thermal transport are both observed to increase during electron cyclotron heating of a high temperature tokamak plasma ($k_\perp$ is the turbulent wavenumber and ρ_i the ion gyroradius). In contrast, large-scale turbulence ($k_\perp \rho_i \leq 1$) and ion thermal transport remain effectively constant. Analysis demonstrates that the small-scale turbulence evolves independently of the ubiquitous, large–scale turbulence and can account for the observed change in electron thermal transport.

1. Introduction

Energy and particle confinement observed in high-temperature tokamak fusion plasmas is often smaller than expected from collisional processes with the deficit attributed to transport arising from micro-instabilities or turbulence [1]. These instabilities include, but are not limited to, ion temperature gradient (ITG) driven modes ($k_\perp \rho_i \sim 0.1$), trapped electron modes (TEM) ($k_\perp \rho_i \sim 1$), and electron temperature gradient (ETG) driven modes ($k_\perp \rho_i \sim 10$) where $k_\perp$ is the fluctuation wavenumber perpendicular to the magnetic field **B** and ρ_i the ion gyroradius. Observations and simulations of low frequency, long wavelength fluctuations are consistent with such instabilities driving thermal and particle transport [1]. However, the current theoretical understanding regarding the role of high frequency, short wavelength modes is much less clear. Theory and simulation have predicted that such modes are capable of either driving significant [2,3] or little [4-7] electron thermal transport (note that Ref. [5] uses low magnetic shear which can affect the resulting transport levels). Experimental measurements are now beginning to approach the high wavenumbers necessary to address these issues [8-12]. Improved, unambiguous measurements across the wavenumber spectrum, particularly at high-k, combined with simultaneous measurement of the transport properties are essential to elucidate understanding in this critical area.

In this paper, the reaction of both large and small-scale density fluctuations to auxiliary plasma heating in the form of electron cyclotron resonance heating (ECH) is described, together with the observed modifications in ion and electron thermal transport. It is found that while the large scale, low-k turbulence levels and ion thermal transport remain approximately constant during ECH, the high-k turbulence levels and electron thermal transport are observed to both increase. This indicates that the high-k fluctuations are not simply remnants of the large amplitude low-k turbulence often reported in the literature [e.g. 13,14]. The observations are also consistent with small-scale turbulence driving at least part of the electron heat transport, since no observed changes occur in other turbulent scales across the plasma. Linear growth rate calculations for these plasmas using gyrokinetic simulation indicate large increases (factors ~2-3) in the growth rates for low-k fluctuations

across the majority of the plasma radius. This is contrary to observations, which indicate little change in fluctuation levels at larger turbulent scales. Somewhat surprisingly, ECH is also found to locally reduce the radial electric field thereby increasing the electric field shearing rate over a broad plasma region to values comparable to the calculated growth rates. Current understanding of shear flow suppression of turbulence [15] suggests that the observed modification in the electric field profile serves to both constrain the growth of low-k fluctuation levels and modify the spectral characteristics in a manner consistent with observations.

2. Experiment and Results

Lower single-null plasmas with $B_T = 1.9$ T, $I_p =$ 700 kA, and chord average density 1.5×10^{19} m^{-3} were used for the results reported here. ECH was initiated at 2000 ms with the injected power increased in a stepwise manner every 300 ms [Fig. 1(a)]. The power from the ECH was deposited in a radially localized volume centered at r/a = 0.6±0.1 with maximum injected power of ~2.4 MW. The plasma electron temperature increased at all measured radii in a stepwise manner similar to the injected ECH [Fig. 1(b)]. In contrast, the ion temperature was not affected by the injected power while the electron density decreased by 10%-20% [Fig. 1(c)]. The decrease in electron density resulted in a change in the density profile shape discussed below. The energy flux and thermal diffusivities associated with ions and electrons was calculated based upon the ECH power deposition location and the measured profiles using the ONETWO transport code [16]. Two different times are shown in Fig. 2 corresponding to no ECH and 2.4 MW ECH power [times 1900 and 3100 ms in Fig. 1(a)]. As seen the ion energy flux did not change appreciably with ECH, consistent with the observed lack of variation in T_i. In contrast, the electron energy flux increased significantly for $r/a > 0.6$ between these two times. It is significant that the ECH dominantly affects the electron energy flux in this plasma parameter regime, having little effect on the ion energy flux.

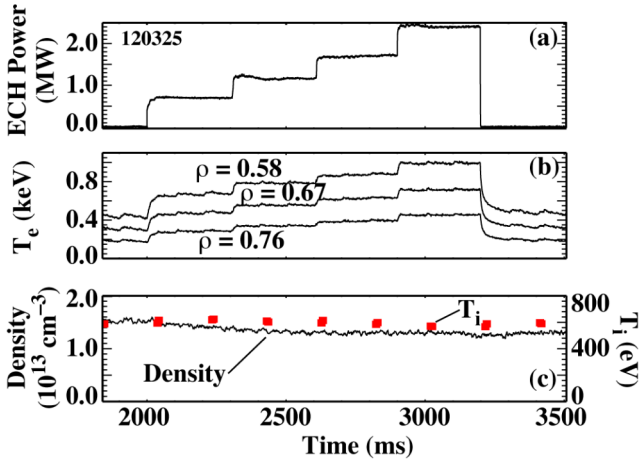

FIG. 1. (a) ECH heating, (b) electron temperature at different radii showing increase with ECH, (c) density and ion temperature ($r/a \sim 0.4$).

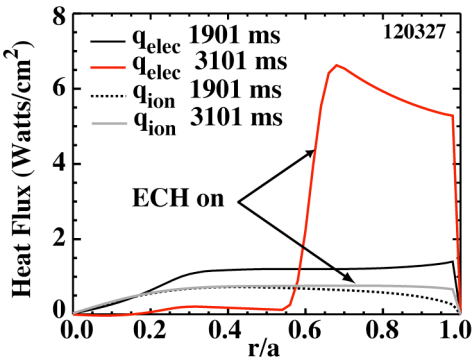

FIG. 2. Electron and ion heat fluxes from two times: Ohmic and ECH heating.

The behavior of the density fluctuations over a broad spectral range was monitored using far-infrared (FIR) scattering and millimeter (mm)-wave backscatter [17]. In addition, reflectometry and beam emission spectroscopy were also employed to locally investigate low-k density fluctuations. The FIR scattering system measures low-k density fluctuations possessing a nearly poloidal wavenumber. The scattered signal is integrated over the wavenumber range 0-2 cm^{-1} with the signal originating from a chord oriented radially along the plasma midplane. The high-k mm-wave backscatter system monitors density fluctuations with a predominately radial wavenumber in the range k = 35-39 cm^{-1}. For the plasmas discussed here this corresponds to a normalized wavenumber range of $k_\perp \rho_i \sim$ 0-0.6 and $k_\perp \rho_i \sim$ 4-10 for the low and high k ranges respectively. The high k signal originates from a chord lying near the midplane which begins at the outboard edge and ends on the low field side at $\rho \simeq 0.4$.

During the high power ECH, low-k fluctuations ($k_\theta \sim$ 0-2 cm^{-1}, from FIR scattering) were observed to decrease in spectral width [Fig. 3(a)] while the integrated amplitude remained approximately constant [Fig. 3(b)]. In contrast to this behavior the high-k fluctuations increase both in frequency width and amplitude during ECH [Fig. 3(c,d)]. The increase in the high-k RMS turbulence level is approximately 15% comparing the two times 1975 and 3100 ms. The very different response of the high and low-k turbulent signals to high power ECH suggests two important conclusions. First, the low and high wavenumber ranges are clearly decoupled, indicating that the small-scale turbulence is not simply a remnant of the large-scale, ITG-like turbulence often observed in tokamak plasmas. Second, the observed increase of high-k fluctuations and the concomitant increase in electron energy transport suggests a causal relationship, especially since large and intermediate-scale fluctuation levels remain effectively unchanged during ECH. In this regard it is interesting to estimate the potential change in the turbulence induced electron heat flux due to the high-k fluctuations. The change in the turbulent electron conductive heat flux $\tilde{q}_e$ is estimated using the observed increase in T_e (~90% at r/a=0.76), the observed increase in $\tilde{n}$ at high k (~15%), and $\tilde{q}_e = n\langle \tilde{T}_e \tilde{E}_\theta \rangle / B \propto n T_e^2 (\tilde{n}/n)^2 / B$ (here the percentage changes in $\tilde{T}_e$ and $\tilde{E}_\theta$ are estimated using the measured changes in $\tilde{n}$). This gives a change in $\tilde{q}_e$ of ~400% suggesting the turbulent heat flux could contribute significantly to the observed change in derived electron heat flux q_e.

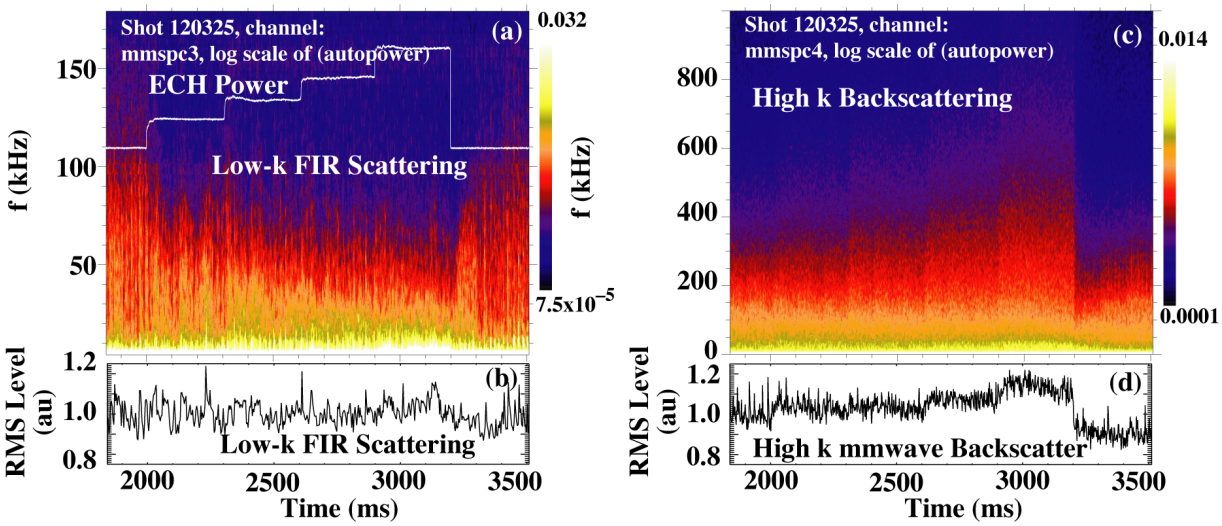

FIG. 3. Low k frequency spectra narrow (a) and fluctuation levels (b) are constant or decrease during ECH. In contrast, high k spectra broaden (c) and fluctuation levels (d) increase.

3. Experiment-Theory Comparisons

In order to compare experimental observations with theoretical expectations, calculations have been performed using the linear gyrokinetic stability code GKS [18]. These calculations indicate that the discharges described in this paper were unstable to a wide range of instabilities: ETG, ITG and TEM. GKS is a gyrokinetic stability code which calculates linear growth rates and frequencies for toroidal drift waves corresponding to poloidal wavenumbers. Code inputs are the measured T_e, T_i, n_e, and Z_{eff} profiles, and magnetic equilibrium. It does not include the effects due to up-down plasma asymmetries or $E \times B$ velocity shear flow (E and B are local electric and magnetic fields). Radial profiles of temperature and density for the two times of interest are shown in Fig. 4(a,b). These are consistent with the time histories shown in Fig. 1 with the electron temperature increasing significantly across the whole radius, and the ion temperature remaining constant. The electron density decreased slightly everywhere except at the very edge. The value of these parameters and their scale lengths are significant inputs into calculations (both analytic and numerical) of various plasma instabilities.

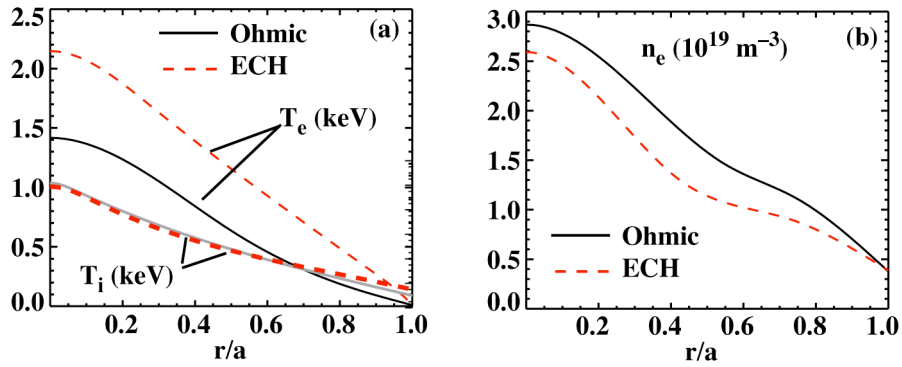

FIG. 4. (a) Ion and electron temperature and (b) density profiles from two times: Ohmic and ECH heating.

Figure 5(a,c) shows the growth rates γ over the radial range ρ = 0.1-0.9 for values relevant to the measured data shown in Fig. 3(a,b) ($\gamma > 0$ indicates instability). It is seen that the plasma is unstable over a range in wavenumber and real space. From Fig. 5(a) it is seen that the low-k growth rate increases significantly during ECH whereas experimentally no change in the fluctuation level was observed [Fig. 3(b)]. Also an increase in real frequency [Fig. 5(b)] is predicted for low k whereas in the experiment a narrowing of the low-k turbulent frequency spectrum was observed. The high-k growth rate increases for r/a > 0.85 but decreases towards the interior. The increased real frequency [Fig. 5(d)] is similar to the observed increase in high-k spectral bandwidth [Fig. 3(c)]. Shown in Fig. 6 are the experimental temperature scale lengths compared to the calculated critical gradient [19] for ETG modes. The experimental gradient is larger than the calculated ETG critical gradient over a large radial range indicating that the calculated high k growth rates [Fig. 5(c)] are consistent with ETG type modes.

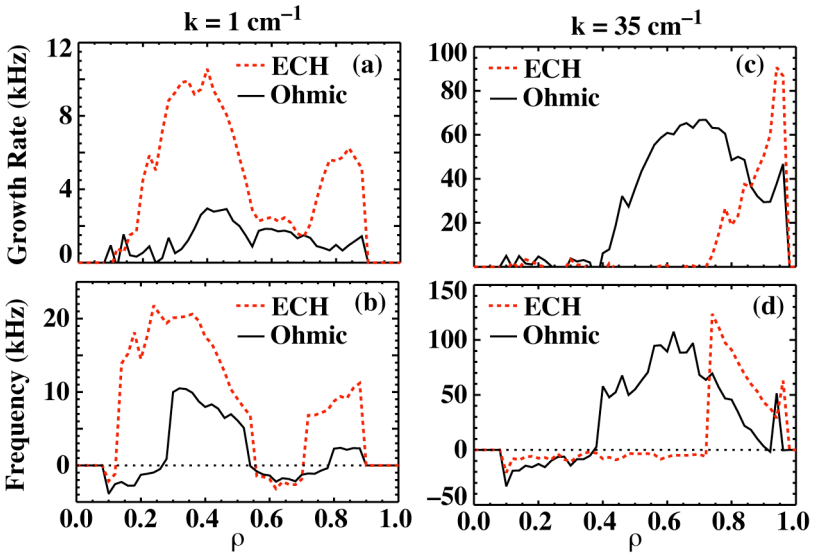

FIG. 5. GKS predictions of growth rates and real frequencies for two different wavenumbers (a,b) 1 cm^{-1} and (c,d) 35 cm^{-1} for two times: Ohmic (solid line) and ECH (dotted line) heating.

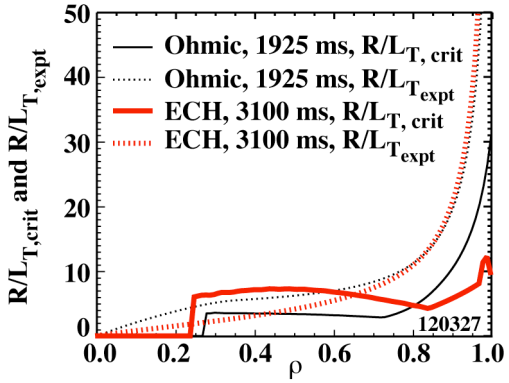

FIG. 6. Comparing SOL of theoretical prediction of ETG critical gradient and experimental gradient. The critical gradient is exceeded for most of the outer half radius in both heating conditions.

Previous theoretical and experimental work indicates that radial electric field shear can lead to significant changes in fluctuations levels and transport [15]. In the experiments here the radial electric field is strongly modified by the ECH shown in Fig. 7(a) where a change is observed for r/a > 0.4. The effect of the ECH is to decrease E_r and to increase the electric field shear around the regions r/a ~ 0.5 and r/a ~ 0.9. The net effect of the reduced electric field strength is to decrease the $E \times B$ velocity Doppler frequency shift of fluctuations as observed in the laboratory reference frame. This agrees well with the observed narrowing in the low-k turbulence frequency spectrum shown in Fig. 3(a). As reviewed in Ref. 15 there is significant evidence that electric field shear can affect low k fluctuations if the shearing rate γ_{ExB} due to shear $E \times B$ velocity flow is a significant fraction of the linear growth rates. Figure 7(b) shows that the shearing rate γ_{ExB} increases over an extended spatial region during ECH. Comparing this value to the value $\gamma_{low\text{-}k}$ from Fig. 5(a) one finds that the shearing rate is a significant fraction of the linear growth rate. This suggests that the predicted increase in low-k turbulence growth rate may be consistent with the observed approximately constant low k fluctuation level if the effect of shearing is taken into account.

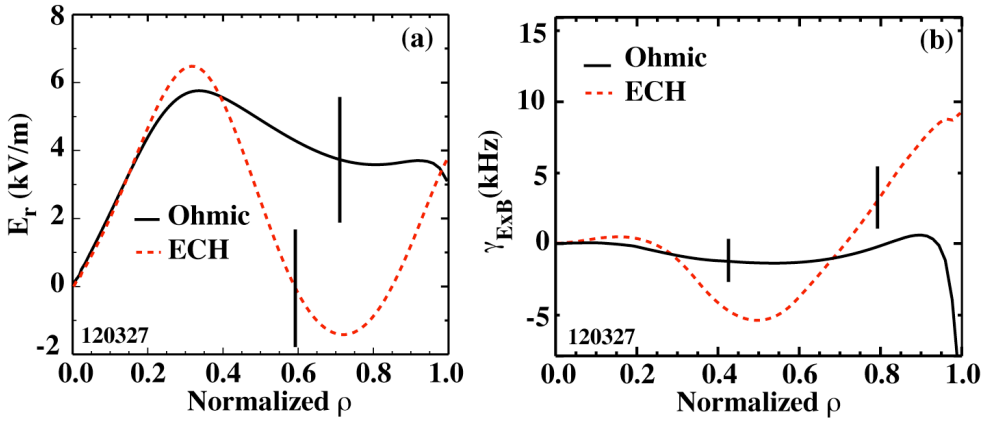

FIG. 7. (a) Electric field and (b) shear shown during Ohmic and ECH time periods. modified by ECH. Typical uncertainties are shown by the vertical bars in (a) and (b).

4. Summary and Conclusion

In summary, high wavenumber ($k_\perp \rho_i$ = 4-10) or electron temperature gradient (ETG) scale plasma turbulence increases in amplitude in the outer plasma region and spectrally broadens during ECH heating of DIII-D Ohmic plasmas. This correlates with an observed increase in electron heat flux in the outer plasma region. In contrast, turbulence at low wave numbers was observed to remain approximately constant in amplitude while the frequency spectrum narrowed. This clearly indicates that the high-k turbulence is not simply a remnant of the low-k turbulence and evolves independently. Linear growth rate calculations at low-k indicate large increases across a broad spatial region during ECH in disagreement with the observed minor modifications in low-k turbulence levels. However, changes in electric field strength and electric field shear are also observed during ECH. These changes provide an explanation for the observed spectral narrowing at low-k and provide a plausible regulation mechanism (i.e. $E \times B$ sheared damping) that balances these increased growth rates at low-k. It should be noted that $E \times B$ shearing is not expected to play an important role at small turbulent scales where a significant increase is observed in the experiment [3].

The results presented in this paper are important especially since recent theoretical work has not fully concluded what role, if any, small-scale turbulence ($k_\perp \rho_i > 4$) plays in governing anomalous electron thermal transport. The data presented indicates that high-k turbulence contributes to electron heat transport in the plasma studied making expansion of such measurements and detailed comparisons to nonlinear gyrokinetic calculations critical to improved understanding.

This work was supported by the U.S. Department of Energy under DE-FG03-01ER54615, DE-FC02-04ER54698, DE-AC05-76OR00033, DE-FG02-89ER53296, and SC6832401.

References

[1] CARRERAS, B.A., IEEE Trans. Plasma Sci. **25**, 1281 (1997); HORTON, W., Rev. Mod. Phys. **71**, 735 (1999).
[2] DORLAND, W., JENKO, F., KOTSCHENREUTHER, M., and ROGERS, B.N., Phys. Rev. Lett. **85**, 5579 (2000).
[3] JENKO, F., and DORLAND, W., Phys. Rev. Lett. **89**, 225001-1 (2002).
[4] LABIT, B., and OTTAVIANI, M., Phys. Plasmas **10**, 126 (2003).
[5] LI, J., and KISIMOTO, Y., Phys. Plasmas **11**, 1493 (2004).
[6] LIN, Z., CHEN, L., and ZONCA, F., Phys. Plasmas **12**, 056125-1 (2005).
[7] GÜRCAN, Ö.D., and DIAMOND, P.H., Phys. Plasmas **11,** 4973 (2004).
[8] PEEBLES, W.A., et al., Proc. 31st EPS Conf. on Plasma Physics (ECA, 2004) Vol. 28G, P-2.174.
[9] WATTERSON, R.L., SLUSHER, R.E., and SURKO, C.M., Phys. Fluids **28**, 2857 (1985).
[10] SAFFMAN, M., et al., Rev. Sci. Instrum. **72**, 2579 (2001).
[11] DEVYNCK, P., et al., Plasma Phys. Control. Fusion **35**, 63 (1993).
[12] TRUC, A., et al., Rev. Sci. Instrum. **63**, 3716 (1992).
[13] RETTIG, C.L., et al., Phys. Plasmas **8**, 2232 (2001).
[14] BROWER, D.L., et al., Phys. Rev. Lett. **59**, 48 (1987).
[15] BURRELL, K.H., Phys. Plasmas **4**, 1499 (1997).
[16] ST JOHN, H., et al., Plasma Phys. and Control. Nucl. Fusion Research **3**, 603 (1966).
[17] RHODES, T.L., et al., "Millimeter-wave Backscatter Diagnostic for the Study of Short Scale Length Plasma Fluctuations," to be published in Rev. Sci. Instrum. (2006).
[18] KOTSCHENREUTHER, M., REWOLDT, G., and TANG, W.M., Comput. Phys. Commun. **88**, 128 (1995).
[19] JENKO, F., DORLAND, W., and HAMMET, G.W., Phys Plasmas **8**, 4096 (2001).